Statistical Shape and Motion Model for Myocardial Deformation from Tagged Magnetic Resonance Imaging

Thalia Eleni Seale, Vicente Grau, Abhirup Banerjee

Institute of Biomedical Engineering, Department of Engineering Science, University of Oxford, Oxford, United Kingdom

Abstract

Abnormal myocardial function is associated with adverse cardiovascular outcomes, including myocardial infarction (MI), but clinical strain measures often reduce complex regional dynamics to just a few metrics. Tagged Magnetic Resonance Imaging (MRI) encodes a spatial reference pattern within the myocardium, enabling direct tracking of tissue deformation and modelling of myocardial material motion, beyond the anatomical shape changes observable in cine MRI. In this work, we propose a principal component analysis (PCA)-based statistical shape and motion model (SSMM) to capture this high-dimensional spatiotemporal variation in myocardial geometry and deformation over the cardiac cycle from tagged MRI-derived motion fields. Using 759 UK Biobank subjects with paired tagged and cine MRI, we fit the SSMM and demonstrate its ability to predict MI with an area under the receiver operating characteristic curve (AUC) of 0.706. We assess model interpretability through qualitative analysis of the modes of variation, revealing deformation patterns unique to tagged MRI that distinguish MI from non-MI subjects. By modelling spatiotemporal myocardial variation, the proposed SSMM provides a data-driven framework for characterising myocardial functional dynamics and their association with disease, with potential to improve disease phenotyping and detection.

1. Introduction

Myocardial function is strongly associated with cardiovascular disease (CVD), with myocardial strain predictive of adverse outcomes. Despite growing evidence that regional and temporal deformation patterns provide additional clinical insight, including in myocardial infarction (MI) [1], standard strain measures are typically summarised as peak values along principal directions (circumferential, radial, and longitudinal), providing a constrained view of myocardial deformation.

Tagged magnetic resonance imaging (MRI) enables direct characterisation of myocardial deformation by encoding tissue tag lines that deform with the myocardium, providing observation of material motion, unlike more prevalent clinical modalities such as cine MRI, which provide more limited measures of deformation. However, recent studies using tagged MRI [2] continue to rely on strain, while data-driven approaches focus on strain estimation and motion tracking [3], rather than modelling full spatiotemporal deformation.

A separate line of work has focused on statistical shape modelling and geometric deep learning of dynamic biventricular anatomy from cine MRI [4]. While effective for modelling anatomical variation, motion is represented using endocardial and epicardial surfaces, with no ability to capture myocardial material deformation.

Overall, despite the rich spatiotemporal information available in tagged MRI, few data-driven approaches model myocardial deformation beyond strain, while cine-based models provide limited access to material motion.

In this work, we characterise regional myocardial deformation throughout the cardiac cycle using tagged MRI. We estimate dense myocardial motion via optical flow, validated against manual tag annotations (average error 1.33 ± 0.99 pixels), and propose a statistical shape and motion model based on principal component analysis (PCA) to capture spatiotemporal variation in myocardial geometry and deformation. We show that SSMM-derived features predict myocardial infarction in 759 UK Biobank subjects (area under the receiver operating curve (AUC) $=$ 0.706), with performance comparable to ejection fraction and cine-derived features, and demonstrate interpretability through latent space analysis. Code and animated figures are available at https://github.com/MultiMeDIA-Oxford/SSMM_myocardial_deformation.

2. Methods

2.1. Dataset

The dataset consists of 759 UK Biobank subjects with paired cine and tagged MRI [5]. Subjects were stratified

into healthy (464), incident myocardial infarction (iMI, 124, subjects who develop MI after imaging), and prevalent myocardial infarction (pMI, 171, subjects with prior diagnosis at imaging time) groups. Cine MRI was processed using [6] to obtain 3D point clouds of the biventricular anatomy. Tagged MRI acquisitions comprised three short-axis slices with 15–30 temporal frames.

2.2. Myocardial Point Cloud Construction

For each subject, myocardial material points were initialised at end-diastole (ED) by fitting a template mesh to point cloud-derived anatomical contours aligned with the tagged MRI slices, enabling consistent point correspondence in the mesh. In-plane motion was estimated from tagged MRI using optical flow (Farnebäck algorithm, Gaussian filtering [7]) to obtain frame-to-frame displacement fields; material points were propagated through time via advection to track myocardial motion. Finally, tracked points were mapped into the normalised cine point cloud space and aggregated across slices to form myocardial point clouds over the cardiac cycle (Figure 1).

2.3. Statistical Shape and Motion Model

The proposed statistical shape and motion model (SSMM) consists of two components: a shape model that encodes myocardial geometry at each time point, and a motion model that captures the temporal dynamics of this geometry. Model pipeline is illustrated in Figure 2.

Shape Model. We denote each myocardial point cloud at time t by $\mathcal{Q}^t = \{\mathbf{p_1^t}, \ldots, \mathbf{p_M^t}\} \subset \mathbb{R}^{\mathbf{3}}$. We represent the point cloud of the nth subject by stacking point coordinates into a feature vector $\mathbf{q}_n^t \in \mathbb{R}^{3M}$. Pooling feature vectors across subjects and time, we apply PCA to obtain a low-dimensional representation of myocardial geometry. Each point cloud is projected onto the leading components as

$$\mathbf{z}_{\text{geom},n}^t = \mathbf{U}^\intercal(\mathbf{q}_n^t - \bar{\mathbf{q}}),$$

where $\mathbf{U}$ contains the leading eigenvectors and $\bar{\mathbf{q}}$ is the mean feature vector.

Motion Model. Let $z_{\text{geom,n}}^{(j)}(t)$ denote the value of latent variable j for subject n at time t. The temporal evolution of this latent variable over the cardiac cycle defines a trajectory,

$$\mathbf{z}_{\text{geom,n}}^{(j)} = \left[z_{\text{geom,n}}^{(j)}(0), \ldots, z_{\text{geom,n}}^{(j)}(T-1)\right]^\intercal \in \mathbb{R}^T.$$

To account for variable temporal sampling across subjects, trajectories are resampled using piecewise cubic Hermite interpolation (PCHIP), yielding $\widetilde{\mathbf{z}}_{\text{geom,n}}^{(j)} \in \mathbb{R}^{\widetilde{T}}$.

A second PCA is then applied across subjects to the resampled trajectories for each component. Specifically, the temporal latent representation is obtained as

$$\mathbf{z}_{\text{temp},n}^{(j)} = \mathbf{V}^{(j)\intercal}\left(\widetilde{\mathbf{z}}_{\text{geom,n}}^{(j)} - \overline{\mathbf{z}}_{\text{geom}}^{(j)}\right),$$

where $\mathbf{V}^{(j)}$ contains the leading temporal eigenvectors and $\overline{\mathbf{z}}_{\text{geom}}^{(j)}$ is the mean trajectory.

2.4. MI Prediction/Detection Model

We evaluated the clinical relevance of the extracted features using ridge regression to predict iMI/pMI from latent encodings. We benchmarked against (i) ejection fraction (EF), and (ii) PCA features from ED and end-systolic (ES) cine anatomies.

3. Results

The shape model was fit on 412 healthy subjects using 30 principal components explaining 98% of shape variance, while the motion model used 5 principal components per shape mode.

3.1. Tag Tracking Validation

We manually tracked myocardial tags in 6 subjects across all slices and cardiac phases. For each tag, the nearest ED point was identified and propagated using optical flow. Performance was assessed by the Euclidean distance between propagated and manually tracked trajectories, yielding a mean error of 1.33 ± 0.99 pixels, below the average tag size of 3 pixels. Error varied with slice location, with lower error in the basal slice (1.18) compared to the apical slice (1.46).

3.2. MI Prediction/Detection

We report prediction results for iMI and pMI in Table 1.

Table 1. Performance of regression models. Population (Pop.) indicates the target (iMI or pMI). Features (Feats.) denote the input representation: proposed method (Ours), PCA features, or EF. Metrics include accuracy (Acc.), AUC, F1-score (F1), precision (Prec.), and sensitivity (Sens.).

Pop.	Feats.	Acc.	AUC	F1	Prec.	Sens.
iMI	Ours	0.787	**0.706**	**0.331**	0.402	**0.287**
	PCA	**0.805**	0.663	0.152	**0.595**	0.094
	EF	**0.805**	0.616	0.029	0.267	0.016
pMI	Ours	0.778	0.766	**0.542**	0.556	**0.529**
	PCA	**0.794**	**0.768**	0.451	**0.700**	0.341
	EF	0.773	0.706	0.320	0.644	0.216

For iMI, the proposed method achieves the highest AUC and F1-score, indicating improved detection performance

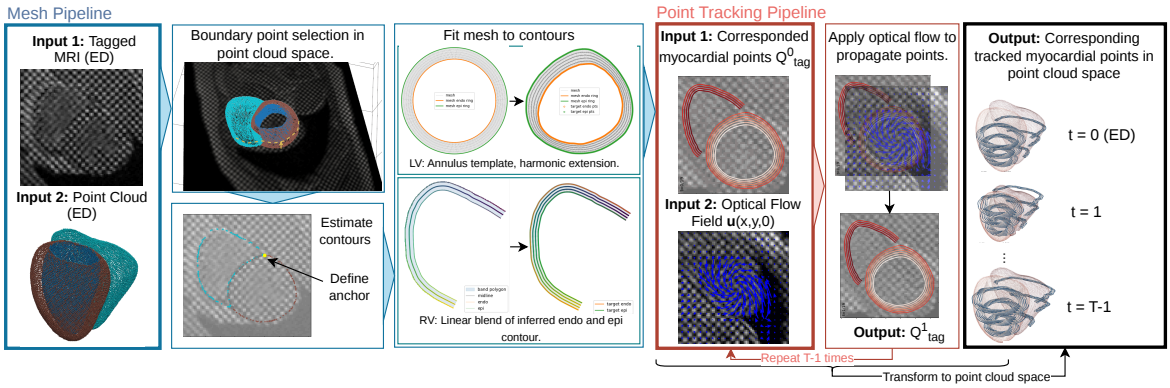

Figure 1. **Preprocessing pipeline.** We fit a mesh to point cloud-derived contours at ED. We then use optical flow to propagate these points throughout the cardiac cycle, and place them in cine point cloud space.

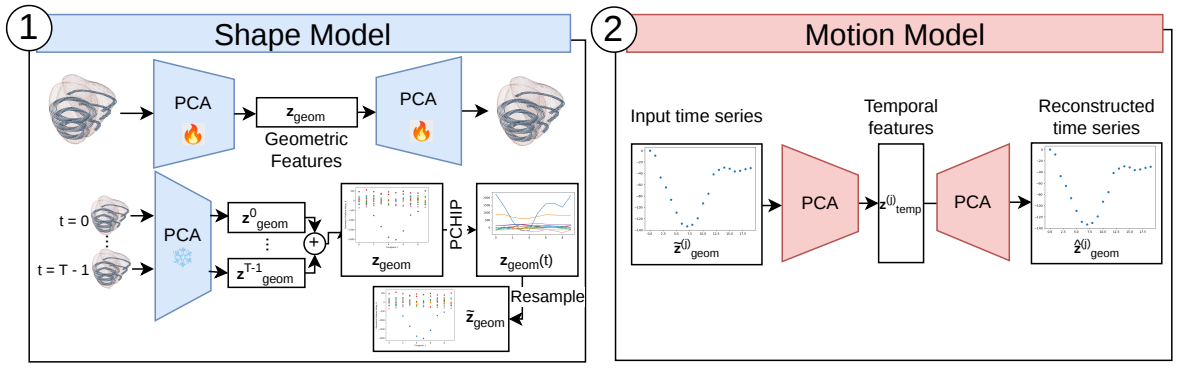

Figure 2. **Overview of the SSMM.** (1) Shape model: Encodes myocardial point clouds to shape features; (2) Temporal features: PCA on resampled trajectories captures key temporal patterns.

compared to baseline approaches, which favour precision at the expense of sensitivity.

For pMI, the proposed method achieves the highest F1-score and sensitivity, while maintaining comparable AUC to PCA, suggesting improved identification of positive cases. Notably, both PCA and EF exhibit lower sensitivity, indicating reduced effectiveness for detection.

3.3. Latent Space Traversal

We provide example latent space traversals of two shape features and associated motion features, illustrating interpretable variations in shape and motion (Figure 3). Motion features shown were significant at the 1% level in a logistic regression predicting iMI/pMI.

4. Discussion

We present a statistical shape and motion model for characterising myocardial deformation from tagged MRI. To our knowledge, this is the first data-driven approach to model three-dimensional myocardial deformation over the cardiac cycle using dense motion information. The learned representation captures both boundary-derived structure and intra-myocardial deformation not accessible from cine MRI. Figure 3 provides a concrete example of this: Mode 8 reveals behaviour not observable in cine imaging, where the region marked ① exhibits predominantly tangential displacement, reflecting material deformation rather than simple boundary motion.

Importantly, the associated motion modes (2, 4) indicate that these patterns reflect meaningful temporal variation rather than artifacts of mesh initialisation, with Mode 8 capturing genuine differences in myocardial deformation.

Mode 28 highlights the model's ability to capture spatially heterogeneous deformation and coordinated behaviour across slices. In the highlighted region ②, deformation differs between slices, with the apical myocardium moving inward while the basal myocardium moves outward relative to the centre at the same phase of the cardiac cycle. This shows that the model captures structured regional variation in deformation, as well as relationships between slices.

Beyond prediction, the model learns a compact latent

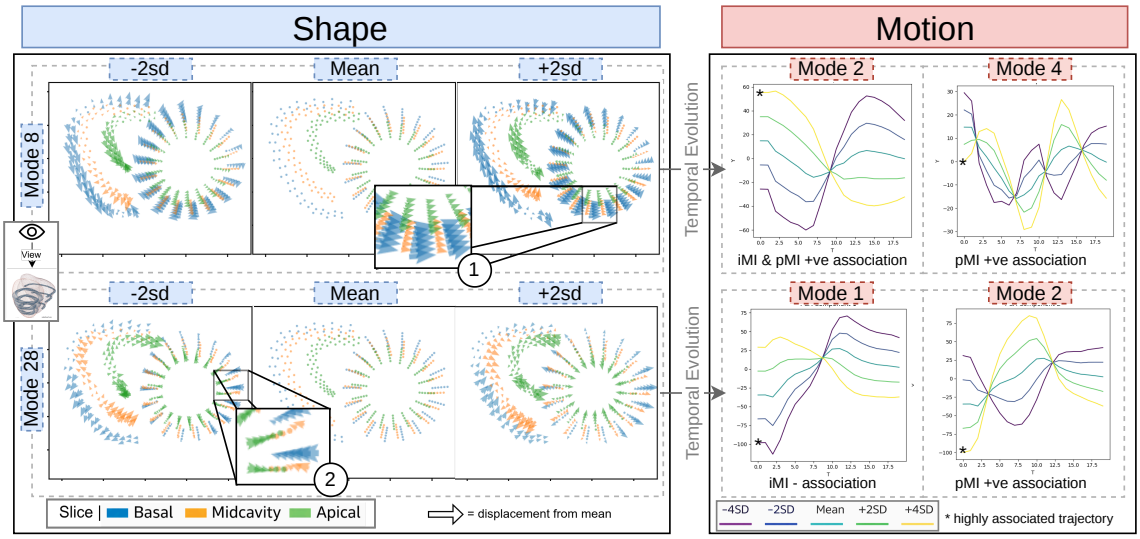

Figure 3. Latent space traversal illustrating the effect of varying individual geometric and temporal components.

representation of myocardial motion that enables generation of physiologically plausible deformation, supporting applications in simulation and personalised modelling.

Although our proposed features improved sensitivity in iMI detection, it remains low. Our analysis used only three slices; if the future infarction lies outside their coverage, any signal may be too weak to detect. This could be improved with a more comprehensive acquisition.

5. Conclusion

This study introduces a PCA-based statistical shape and motion model to quantify biventricular myocardial function throughout the cardiac cycle. The proposed features achieve competitive performance for myocardial infarction prediction and provide an interpretable representation of myocardial deformation. Key latent features capture clinically relevant patterns, including localised, non-uniform thickening and distinct temporal behaviour between iMI and pMI, highlighting the value of modelling dense spatiotemporal myocardial function beyond conventional summary metrics.

Acknowledgments

This research has been conducted using the UK Biobank Resource under Application Number ‘40161’. The authors express no conflict of interest. TS is supported by the EPSRC Centre for Doctoral Training in Health Data Science (EP/S02428X/1). AB is supported by the Royal Society University Research Fellowship (Grant No. URF\R1\221314).

References

[1] Bhalodiya JM, et al. Identifying myocardial infarction using hierarchical template matching–based myocardial strain: Algorithm development and usability study. JMIR Medical Informatics 2021;9(2):e22164.

[2] Ng MY, et al. Diagnostic accuracy of cardiovascular magnetic resonance strain analysis and atrial size to identify heart failure with preserved ejection fraction. European Heart Journal Open 2023;3(2):oead021.

[3] Abd-Elmoniem KZ, et al. Direct pixel to pixel principal strain mapping from tagging MRI using end to end deep convolutional neural network (DeepStrain). Scientific Reports 2021;11(1):23021.

[4] Qiao M, et al. A personalized time-resolved 3D mesh generative model for unveiling normal heart dynamics. Nature Machine Intelligence 2025;7(5):800–811.

[5] Petersen SE, et al. UK Biobank’s cardiovascular magnetic resonance protocol. Journal of Cardiovascular Magnetic Resonance 2016;18(1):8.

[6] Beetz M, et al. Multi-class point cloud completion networks for 3D cardiac anatomy reconstruction from cine magnetic resonance images. Medical Image Analysis 2023;90:102975.

[7] Farnebäck G. Two-frame motion estimation based on polynomial expansion. In Proceedings of the 13th Scandinavian Conference on Image Analysis, SCIA’03. Berlin, Heidelberg: Springer-Verlag. ISBN 3540406018, 2003; 363–370.

Address for correspondence:

Thalia Eleni Seale
Institute of Biomedical Engineering, Old Road Campus Research Building, Oxford, OX3 7DQ, UK
thalia.seale@eng.ox.ac.uk